Vibrational Energy Gain in the ν_2 Bending Mode of Water via Collisions with Hot Pyrazine (E_{vib} = 37900 cm^{-1}): Insights into the Dynamics of Energy Flow†

Michael S. Elioff, Rebecca L. Sansom, and Amy S. Mullin*

Department of Chemistry, Arthur G. B. Metcalf Center for Science and Engineering, Boston University, Boston, Massachusetts 02215

Received: April 14, 2000; In Final Form: June 19, 2000

Energy gain into specific rotational levels of vibrationally excited $H_2O(010)$ resulting from collisions with highly vibrationally excited pyrazine in a low-pressure, 298 K environment was investigated using high-resolution transient infrared absorption spectroscopy of water at $\lambda \approx 2.7$ μm. Vibrationally excited pyrazine with 37900 cm^{-1} internal energy was generated by 266 nm optical excitation to an electronically excited singlet state of pyrazine, followed by rapid radiationless decay to the ground electronic state. Collisions between highly excited pyrazine and water that result in excitation of the ν_2 bending vibrational mode (ν_2 = 1594 cm^{-1}) in water were studied by monitoring the time-resolved appearance of individual rotational states of $H_2O(010)$. Transient absorption signals were obtained for a number of rotational states with $E_{rot} \leq 811$ cm^{-1}. The nascent distribution of rotational states for the scattered, vibrationally excited water molecules, $H_2O(010)$, is well characterized by a Boltzmann rotational temperature of $T_{rot} = 630 \pm 90$ K. Doppler-broadened transient absorption line shapes for a number of rotational levels within the (010) vibrational state were measured with recoil velocity distributions that correspond to $T_{trans} = 490 \pm 70$ K, independent of rotational state. Bimolecular rate constants and Lennard-Jones probabilities for energy transfer into specific quantum states of $H_2O(010)$ from collisional deactivation of hot pyrazine were determined as well. Our observations for vibrational energy gain in H_2O following collisions with hot pyrazine are compared to earlier studies on collisional energy gain in CO_2. The molecular properties of the energy acceptor that influence the relaxation of highly vibrationally excited molecules are explored and insights into the mechanism for vibrational energy gain in water are presented.

Introduction

Collisional energy transfer plays a significant role in a diverse range of processes including combustion, chemistry in high-temperature environments, chemical lasers, and unimolecular reactions.[1] Extensive research efforts of the 1950s through the 1970s have resulted in a solid understanding of vibrational energy transfer for small molecules with low amounts of vibrational excitation. Much of our understanding today comes from the pioneering work by the groups of Brad Moore, George Flynn, Charlie Parmenter, and others. Over the past 2 decades, research efforts have turned toward quantifying and understanding the collisional deactivation of highly vibrationally excited polyatomic molecules, particularly those with chemically significant amounts of energy. Studies that investigate energy loss from highly excited donor molecules find that water is especially efficient at removing internal energy from excited collision partners.[2−4] We have taken a state-resolved approach to measure the energy gain dynamics for water molecules that are excited through collisions with highly vibrationally excited donor molecules, such as pyrazine and pyridine, to identify the predominant energy transfer pathways that are responsible for water's enhanced ability to remove energy from hot donors. In recent quenching studies of hot pyrazine and pyridine, we investigated the rotational and translational energy gain distributions for water in its (000) vibrationless ground state.[5,6] In this paper, we turn our attention to *vibrational* energy gain in water and report on the state-resolved energy gain dynamics associated with collisional excitation of the ν_2 bending mode (ν_2 = 1594 cm^{-1}) that results from quenching of highly vibrationally excited pyrazine (E_{vib} = 37900 cm^{-1}). One goal of this study is to establish how vibrational energy gain in water contributes to the overall collisional relaxation of highly excited pyrazine with water vapor. Another goal is to compare the energy gain dynamics for water with those for CO_2, where extensive state-resolved studies have already been performed. From this, we hope to elucidate the molecular reasons that determine quenching efficiencies for different bath molecules and provide input for future theoretical descriptions of high-temperature chemical and collisional processes.

State-resolved studies of energy gain in bath molecules are starting to provide the level of detail about specific energy flow pathways in bimolecular collisions that is necessary to reveal the underlying mechanisms for the observed bulk behavior. State-resolved energy gain measurements such as those performed in both the Flynn labs and our labs provide information about the microscopic mechanisms of energy transfer and hence are complementary to both average energy loss studies and kinetically controlled ionization studies that monitor appearance of low energy quenched donors. Studies that monitor collisional energy loss from highly excited donor molecules[7−13] in relatively low-pressure environments find that the average amount of energy $\langle \Delta E \rangle$ transferred from the hot donor molecule is influenced, in general, by two factors. The first of these is that the amount of energy lost per collision, on average, increases

† Part of the special issue "C. Bradley Moore Festschrift".

10.1021/jp001425a CCC: $19.00
Published on Web 07/26/2000

as the internal energy of the hot donor is increased. Energy-dependent state-resolved studies from our lab have provided insight into how specific energy transfer pathways are influenced by the donor internal energy.[14] A second factor that is considered important in determining the efficiency of energy loss from highly vibrationally excited donors is the complexity (or size) of the energy-accepting bath molecule. In this way, Ne is more efficient than He for quenching highly vibrationally excited donors, and polyatomic bath molecules such as CO_2 and H_2O are more efficient than atomic baths. However, there are some deviations from this general rule, particularly for bath molecules containing one or more hydrogen atoms. As an example, CO_2 and H_2O are of comparable molecular complexity but water is generally 1.5−3 times more efficient overall at removing energy from highly excited donors than is CO_2. For the collisional quenching of excited benzene ($E_{vib} = 24000$ cm^{-1}), Barker and co-workers[7] observed that the average energy loss per collision in a CO_2 bath is $\langle \Delta E \rangle = 208$ cm^{-1}, whereas for quenching by H_2O, $\langle \Delta E \rangle = 373$ cm^{-1}. Even more pronounced differences for CO_2 and H_2O quenching efficiencies have been reported by Weisman and co-workers[15] for relaxation of vibrationally excited triplet pyrazine ($E_{vib} = 5000$ cm^{-1}). From a state-resolved perspective, rotational and translational excitation of both $H_2O(000)$[5] and $CO_2(00^00)$[16−18] has been shown to be important in the relaxation of highly excited pyrazine. However, details of the energy gain profiles and probabilities for both quenchers indicate that this pathway alone does not account for water's enhanced efficiency. Thus, additional energy transfer pathways must be important for the collisional relaxation of highly excited donors with water. In this paper, we present the first state-resolved study that investigates the energy transfer dynamics associated with vibrational energy gain in water molecules following collisions with highly vibrationally excited pyrazine.

Experimental Section

All data presented here were collected using the high-resolution transient infrared absorption spectrometer that has been described previously.[5,6] Optical excitation of pyrazine with the frequency-quadrupled output of a pulsed Nd:YAG laser ($\lambda = 266$ nm) was used to prepare electronically excited pyrazine, which subsequently undergoes rapid radiationless decay via the triplet state to the ground electronic state in approximately 50 ns[19,20] with near unity quantum yield.[21] This results in vibrationally excited, electronic ground-state pyrazine molecules with 37900 cm^{-1} of internal energy. A 1:1 mixture of pyrazine and water at $T = 298$ K, and a total pressure of ∼20 mTorr, was introduced into a 250 cm flowing-gas collision cell. The UV beam was propagated collinearly with the continuous wave (cw) IR probe beam, which is described below. Under these experimental conditions, the vibrationally excited pyrazine comprises about 15% of the total pyrazine concentration, and the mean collision time is $t_{col} \approx 4$ μs. The UV power density was kept below 5 MW/cm^2 to minimize multiphoton absorption.

Transient infrared absorption was used to measure the nascent populations of scattered water molecules in specific rotational levels of the (010) state. The IR probe was the tunable output of an F-center laser (FCL) ($\lambda = 2.5$ to 2.8 μm) that was optically pumped by a Krypton ion laser ($\lambda = 647$ nm). Continuous frequency tuning was accomplished in the following way.[5,22] An intracavity diffraction grating allowed coarse frequency selection and single-mode output was achieved through the use of an intracavity étalon that was actively locked to a single cavity mode. The bandwidth of the resulting IR light was 0.0003 cm^{-1}. A pair of intracavity calcium fluoride plates mounted on galvanometers were rotated for fine adjustment of the output frequency, and the intracavity étalon was scanned synchronously to maintain single cavity mode operation. Beam diagnosis was achieved by passing ∼4% of the IR output beam through a scanning Fabry−Perot étalon and monitoring the signal on a photodiode.

All transient absorption signals were collected on a liquid nitrogen cooled InSb detector as a function of time relative to the pulsed UV excitation of pyrazine. The transmitted IR intensity I_{DC} was collected after the IR beam had passed through the collision cell and a monochromator tuned to the frequency of the probe transition. The response of the detector was amplified by a low-noise, high-gain transimpedance amplifier and recorded by a 200-MHz DC-coupled digitizing oscilloscope. The amplified detector signals had a rise time of 100 ns. These signals were transferred to a computer for background correction and analysis. The transient absorption data from 120 ns to 3.0 μs were fit to an exponential function of the form $\Delta I/I_0 = A(1 - e^{-bt})$ and the fit value of $\Delta I/I_0$ at 1 μs following UV excitation was used, as described below, to determine the state specific number density of $H_2O(010,J_{KaKc})$.

To determine the number of scattered water molecules in a particular rotational level of the (010) state, it is necessary to measure both relative peak intensities and absolute line widths for the transitions of interest. Specific rotational states of interest were located using a wavemeter with a resolution of 0.01 cm^{-1}. For line width measurements, the laser was locked to a single cavity mode near the peak of the probe transition, and transient absorption signals were collected as the laser frequency was tuned over the entire transition line profile. The frequency-dependent absorption signals at $t = 1$ μs were fit to a Gaussian function to determine the line width. Peak intensity measurements were performed in a similar way, except that the probe laser was scanned only over the top of the probe transition. The intensity at line center was determined by fitting the frequency-dependent absorption signals at $t = 1$ μs to a Gaussian function to identify the absorption maximum. This approach was used rather than the direct external locking method reported previously[5,6] because the low equilibrium populations of $H_2O(010)$ at 300 K and inefficient collisional excitation of the (010) state in a plasma make it difficult to observe vibrationally excited water molecules in a reference cell.

We must extract the fractional change in IR transmittance due to molecular absorption from these raw signals. The desired information is contained in the DC-coupled signal of the InSb detector, denoted I_{DC}. However, this signal is also influenced by IR intensity fluctuations. The measured signal I_{DC} is given by $I_{DC}(t) = I(t)T(t)$, where $I(t)$ is the pre-cell laser beam intensity, and $T(t)$ is the transmitted intensity due to transient molecular absorption. A similar 100 ns rise time detector and amplifier was used to measure a fraction of the pre-cell laser intensity I_{ref} for each UV laser pulse. The intensity, as a function of time, was fit to a fourth order polynomial and scaled to the I_{DC} signal using $I(t) = I_{ref}(t)I_{DC}(t < 0)/I_{ref}(t < 0)$, where $t = 0$ is defined by the UV laser pulse. The transmitted infrared intensity is therefore related to the detector signals by $T(t) = \{I_{DC}(t)I_{ref}(t < 0)\}/\{I_{ref}(t)I_{DC}(t < 0)\}$. The populations of $H_2O(010)$ in specific rotational quantum states were determined using our experimentally acquired IR transmission values $T(t)$, the absorption strengths from the HITRAN high-temperature spectral database,[23] and the Beer−Lambert law.

The water used in these experiments was fractionally distilled and sealed in a vacuum flask at 100 °C to prevent absorption

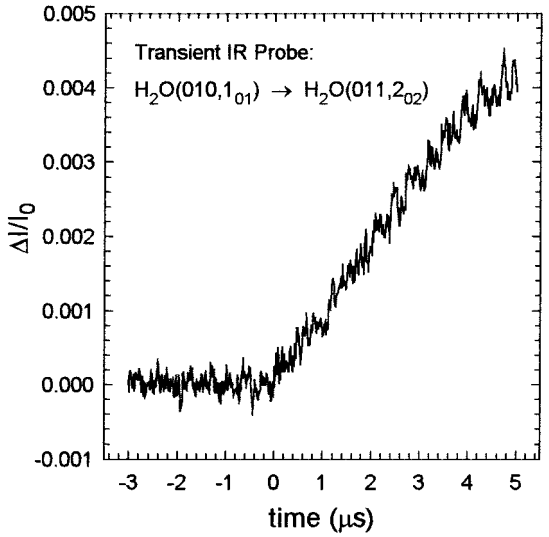

Figure 1. Fractional transient absorption of $H_2O(010,1_{01})$ resulting from collisions with vibrationally excited pyrazine (E_{vib} = 37900 cm^{-1}) measured as a function of time with respect to pulsed excitation of pyrazine at 266 nm. The total cell pressure is ~20 mTorr and the cell temperature is T = 298 K. Typical transient signals are collected and averaged over 250 UV laser shots.

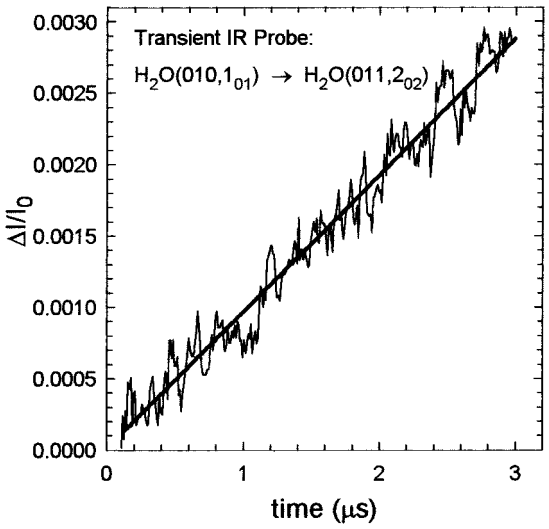

Figure 2. Fractional transient absorption of $H_2O(010,1_{01})$ resulting from collisions with vibrationally excited pyrazine (E_{vib} = 37900 cm^{-1}) measured as a function of time after UV excitation of pyrazine. The transient signal is shown as a thin line and the fit to $y = A(1 - e^{-bt})$ from t = 120 ns to 3.0 μs is shown as a thick solid line, demonstrating the linearity of the signal at early times.

of atmospheric gases. The pyrazine was of research quality (Aldrich 99+%), and was degassed by several freeze/pump/thaw cycles.

Results

1. Transient Infrared Absorption of $H_2O(010)$. The temporal evolution of rotational state populations of nascent $H_2O(010)$ molecules resulting from collisions with highly vibrationally excited pyrazine was monitored using high-resolution laser transient infrared absorption. The appearance of specific rotational states of $H_2O(010)$ with rotational energies ranging from 23 to 811 cm^{-1} was probed using the strongly allowed asymmetric stretch transition near 3756 cm^{-1},

$$H_2O(010,J_{KaKc}) + h\nu(\lambda \approx 2.7\ \mu m) \rightarrow H_2O(011,J'_{Ka'Kc'})$$

where J is the total rotational angular momentum quantum number and K_a and K_c are the limiting symmetric top projection quantum numbers. For water, rotational states for which the sum of K_a and K_c is odd are referred to as "ortho" states and have a nuclear spin degeneracy of g = 3. States for which the sum of K_a and K_c is even are referred to as "para" states and have a nuclear spin degeneracy of g = 1. Figure 1 shows the transient infrared absorption signal corresponding to the appearance of population in $H_2O(010,1_{01})$ which results from collisions with highly excited pyrazine (E_{vib} = 37900 cm^{-1}) prepared by pulsed UV excitation at t = 0 μs. The transient signal for this state was collected using the $H_2O(010,1_{01}) \rightarrow H_2O(011,2_{02})$ probe transition. It is worth noting that the absorption strength for the 010 → 011 transition in water is approximately four times less intense than is the 000 → 001 transition, which was used in earlier studies on water from our lab.[5,6] This fact and reduced energy transfer probabilities for the (010) state account for the reduced signal-to-noise ratio in the present study. In Figure 2, we present the results of an exponential fit to the transient absorption data (as described in the Experimental Section), which is linear to $t \sim 3$ μs and has zero amplitude at t = 0. These features demonstrate that data collected prior to $t \sim 3$ μs result from energy transfer occurring from single encounters between hot pyrazine and water. This is consistent with the average time between collisions of $t_{col} \approx 4$ μs for our experimental conditions with a total cell pressure of 20 mTorr and T = 298 K.

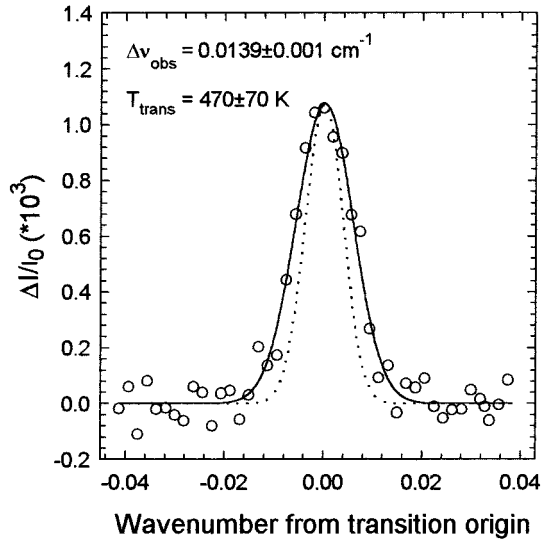

Figure 3. Transient absorption line profile for $H_2O(010,3_{03})$ collected 1 μs following UV excitation of vibrationally excited pyrazine (E_{vib} = 37900 cm^{-1}). The transient absorption data, shown as open circles, are fit to a single Gaussian function, shown as a solid line. This fit yields a full width at half-maximum line width of $\Delta\nu_{obs}$ = 0.0139 ± 0.001 cm^{-1}, which corresponds to a lab-frame translational temperature of 470 ± 70 K. The transient line width is broadened relative to the initial 298 K line profile, which is shown as a dotted line for comparison.

2. Translational Energy Gain in Scattered $H_2O(010)$. Distributions of nascent recoil velocities accompanying energy gain into rotational states of $H_2O(010)$ were obtained by determining transient Doppler-broadened line shapes for individual rotational states of $H_2O(010)$. The populations of individual rotational levels within the (010) vibrational state of water were measured 1 μs after UV excitation of pyrazine and collected as a function of infrared frequency shift $\delta\nu$ from the transition origin. Figure 3 depicts a transient line profile for the $H_2O(010,3_{03})$ state. The experimental data in Figure 3, shown as circles, were fit to a Gaussian line shape using a nonlinear

TABLE 1: Nascent Doppler-Broadened Line Widths and Corresponding Translational Temperatures for Energy Transfer from Vibrationally Excited Pyrazine to Water via the Collision Process: Pyr(E_{vib} = 37900 cm^{-1}) + H_2O → Pyr(E_{vib} − ΔE) + H_2O(010, J_{KaKc})

H_2O(010) J_{KaKc}	transition frequency[a]	E_{rot}[b]	$\Delta\nu_{obs}$[c]	T_{trans}[d]	$E_{trans,lab}$[e]	$\Delta E_{trans,rel}$[f]
1_{01}	3782.180	23.811	0.0143 ± 0.001	510 ± 80	530 ± 80	260 ± 40
3_{03}	3818.775	137.150	0.0139 ± 0.001	470 ± 70	490 ± 70	210 ± 30
3_{21}	3654.321	224.589	0.0147 ± 0.001	560 ± 90	580 ± 90	330 ± 50
5_{05}	3850.307	326.021	0.0135 ± 0.001	430 ± 60	450 ± 70	170 ± 30

[a] The transition energy, in cm^{-1}, of the H_2O(010) probe, from ref 23. [b] The energy, in cm^{-1}, of the H_2O(010) rotational state J_{KaKc} from ref 23. [c] Transient absorption line width, in cm^{-1}, measured 1 μs after UV excitation of pyrazine. [d] Translational temperatures for individual rotational states of water are determined from line width measurements using the relationship $T(K) = (mc^2\Delta\nu_{obs}^2)/(8R\ln(2)\nu_0^2)$, where m is the mass of water, R is the gas constant, and ν_0 is the transition frequency, in cm^{-1}. [e] Average lab-frame translational energy, in cm^{-1}, of H_2O(010) molecules scattered from highly vibrationally excited pyrazine, found using $E_{trans,\,lab} = 1.5k_BT_{trans}$. [f] Average change in the center-of-mass translational energy, in cm^{-1}, of the system consisting of recoiling H_2O(010) molecules and pyrazine molecules determined using the relationship $\Delta E_{trans,rel} = [(m_w + m_p)/m_p]\Delta E_{lab} = 1.22\Delta E_{trans,lab}$ where T_0 = 298 K, as described in the text.

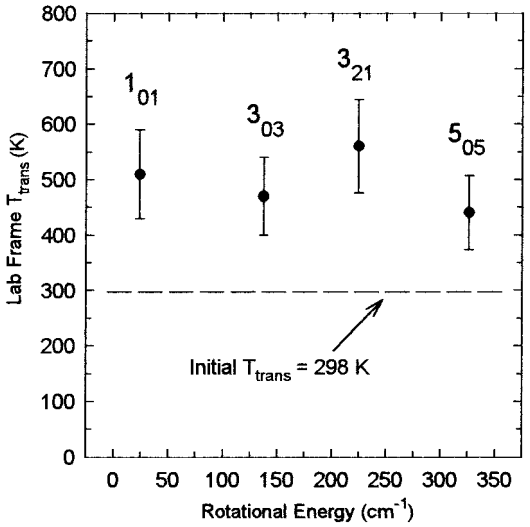

Figure 4. Nascent translational temperatures for individual rotational states of H_2O(010) with rotational energies between 23 and 350 cm^{-1}. Translational temperatures are determined by measuring Doppler-broadened line widths 1 μs following UV excitation of pyrazine. All transient line widths are broadened relative to the initial line widths at 298 K and no increase of translational temperature with final J_{KaKc} state was observed. The reported error is determined using an uncertainty of ±0.001 cm^{-1} in the experimental line widths.

least-squares analysis. The solid line represents the Gaussian fit of the data and the dotted line represents the room temperature (298 K) line shape. The observed full width at half-maximum (fwhm) for the 3_{03} rotational state is $\Delta\nu_{obs}$ = 0.0139 ± 0.001 cm^{-1}. This state exhibits modest line shape broadening relative to the initial 298 K line width of $\Delta\nu_{298}$ = 0.0109 ± 0.001 cm^{-1} and corresponds to a lab-frame translational temperature of T_{trans} = 470 ± 70 K. The translational temperatures for individual rotational states are determined using the relationship

$$T_{trans} = \frac{mc^2}{8R\ln(2)}\left(\frac{\Delta\upsilon_{obs}}{\upsilon_0}\right)^2$$

where m is the mass of water in kg mol^{-1}, c is the speed of light in m s^{-1}, R is the gas constant in J mol^{-1} K^{-1}, $\Delta\nu_{obs}$ is the experimental fwhm line width and ν_0 is the frequency of the probe transition in cm^{-1}. Transient line widths for four different rotational states of H_2O(010) were measured and, as shown in Table 1 and Figure 4, correspond to translational temperatures ranging from T_{trans} = 560 K for the 3_{21} state to T_{trans} = 430 K for the 5_{05} state. From these values, average translational energies for the scattered water molecules have been determined using the expression $E_{trans} = {}^3/_2k_BT_{trans}$, where k_B is Boltzmann's constant. The average translational energies of the scattered H_2O(010) rotational states are about twice their initial values at 298 K, indicating that the vibrationally hot water molecules also gain some translational energy during their encounters with hot pyrazine. In addition, the recoil velocity distributions do not depend systematically on the rotational energy of H_2O(010). It is noteworthy that a similar lack of rotational dependence in the recoil energies was observed for the ground vibrationless state of water. This will be discussed later.

It is useful to consider the amount of energy lost from the hot pyrazine that goes into translational energy between the recoiling molecules. In the lab frame, the change in average translational energy is given by $\Delta E_{trans,lab} = {}^3/_2k_B(T_{trans} - T_0)$, where T_0 describes the initial translational energy distribution. By transforming the velocity distributions into the center of mass frame for an isotropic distribution of recoiling water molecules, the pyrazine internal energy that is transformed into recoil between pyrazine and water is given by $\Delta E_{trans,rel} = [(m_w + m_p)/m_p]\Delta E_{trans,lab} = 1.22\Delta E_{trans,lab}$. In this expression, m_w and m_p are the masses of water and pyrazine, respectively. These values are between ΔE_{rel} = 170−330 cm^{-1}, as listed in Table 1. Thus, the vibration-to-translation energy exchange associated with excitation of the (010) state of water represents only a small part of the pyrazine initial energy (E_{vib} = 37900 cm^{-1}).

3. Rotational Excitation of H_2O(010). Nascent rotational populations of water molecules scattered into the (010) vibrational state were obtained by measuring the transient absorption for a number of rotational states in the (010) state at t = 1 μs following UV excitation of pyrazine and integrating over the experimentally determined line widths, as described above. In cases where line widths were not measured, an average translational temperature T_{trans} = 490 K was used. The distribution of rotational states for scattered H_2O(010) molecules following collisions with hot pyrazine is determined by dividing each state-specific population by the nuclear spin degeneracy[24] of that state and plotting the natural logarithm of this quotient as a function of the rotational energy, as shown in Figure 5. This analysis results in a rotational distribution that is well described by T_{rot} = 630 ± 90 K. Thus, collisions that put energy into the (010) bending state of water are also accompanied by rotational and translational excitation.

4. Rate Constants for Energy Transfer to the H_2O(010) State. We now present measurements of the absolute probability for energy gain into the (010) state of water that results from the collisional quenching of highly excited pyrazine with H_2O. The probability P that a bimolecular collision will have a particular energy transfer outcome is defined as the ratio of the state-specific energy transfer rate to the collision rate, i.e., $P = k_2^J/k_{col}$. In this section, we report state-specific bimolecular

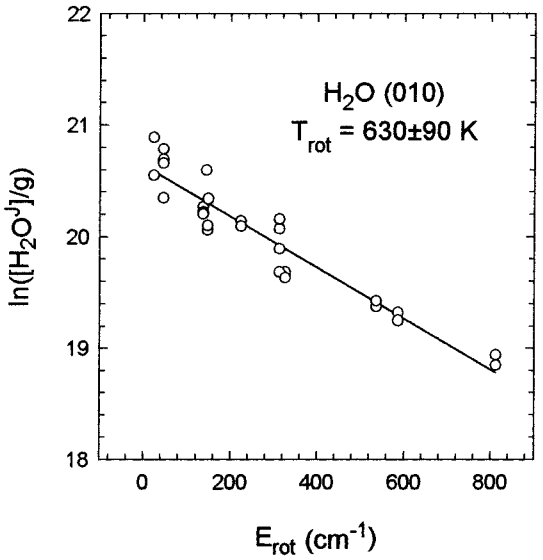

Figure 5. Nascent rotational populations for individual rotational states (E_{rot} = 23 to 811 cm^{-1}) of scattered $H_2O(010)$ measured 1 μs after UV excitation of pyrazine (E_{vib} = 37900 cm^{-1}). The rotational distribution is well characterized by a Boltzmann temperature of 630 ± 90 K, with a non-least-squares linear regression analysis r^2 value of 0.91.

energy transfer rate constants k_2^J for the process:

$$\mathrm{Pyr}(E_{vib} = 37900\ \mathrm{cm}^{-1}) + \mathrm{H_2O} \xrightarrow{k_2^J} \mathrm{Pyr}(E_{vib} - \Delta E) + \mathrm{H_2O}(010, J_{KaKc})$$

The appearance of water (010) molecules in individual rotational states J_{KaKc} resulting from collisions between excited pyrazine and a 298 K bath of water are monitored using infrared absorption. We measure state-specific $H_2O(010)$ populations 1 μs following UV excitation. By measuring the populations at times much shorter than the average collision time (~4 μs), the effects of subsequent collisions and migration of scattered water molecules out of the path of the probe laser beam are minimized. Under these conditions, the early-time appearance of rotationally excited states of water may be expressed as

$$\frac{\mathrm{d}[\mathrm{H_2O}(010, J_{KaKc})]}{\mathrm{d}t} = k_2^J[\mathrm{Pyr}^*][\mathrm{H_2O}]$$

where [Pyr*] represents the concentration of vibrationally excited pyrazine and [H_2O] is the bulk concentration of the water. Immediately following UV excitation, the concentration of bulk water is much greater than the scattered water, so [H_2O] at $t = 0$ may be treated as a constant, $[H_2O]_0$. Moreover, given the linearity demonstrated in Figure 2, it is reasonable to assume that the vibrationally excited pyrazine concentration is essentially unchanged for the first microsecond, so that the early time [Pyr*] may also be treated as a constant defined by the $t = 0$ excited pyrazine concentration, $[Pyr^*]_0$. At the UV powers used in these experiments, we estimate that two-photon absorption accounts for less than 7% of the excited pyrazine population. Therefore, to a very good degree of accuracy, the initial concentration of excited pyrazine $[Pyr^*]_0$ is given by the number of UV photons absorbed per cm^3 in the interaction region. The energy transfer rate constants for appearance of individual quantum state of $H_2O(010)$ can therefore be expressed as

$$k_2^J = \frac{[\mathrm{H_2O}(010, J_{KaKc})]}{[\mathrm{Pyr}^*]_0[\mathrm{H_2O}]_0 t}$$

where $t = 1$ μs. Table 2 presents rate constants for energy gain into specific rotational levels of $H_2O(010)$ that result from collisions with hot pyrazine. These rate constants decrease as a function of increasing rotational energy and range from 3.5 × 10^{-13} cm^3 molecule^{-1} s^{-1} for the appearance of the (010, 1_{01}) state to 4.8 × 10^{-14} cm^3 molecule^{-1} s^{-1} for the appearance of the (010, 5_{50}) state.

It is useful for comparison purposes to obtain an overall rate constant for excitation of the (010) vibrational state. An expression for the total rate constant associated with the excitation of into the $H_2O(010)$ state is found by integrating over the observed rotational distribution. The integrated energy transfer rate constant for excitation of the (010) state is therefore given by

$$k_2^{INT} = \sum_{E=0}^{811} k_2^J = (4.95 \pm 0.98) \times 10^{-12}\ \mathrm{cm^3\,molecule^{-1}\,s^{-1}}$$

where we have used the data in Table 2 and Figure 5 to interpolate for states that were not measured and summed the rate constants for energy gain into all H_2O (010, J_{KaKc}) states with rotational energies up to 811 cm^{-1}, the highest rotational energy for which we observe scattering. In Figure 6, the experimentally measured energy transfer rate constants are plotted as a function of rotational energy along with the exponential fit to a Boltzmann distribution.

To determine energy transfer probabilities, it is necessary to define a collision rate constant, k_{col}. The hard sphere collision rate constant for pyrazine and water at 298 K is k_{HS} = 3.3 × 10^{-10} cm^{3}molecule^{-1}s^{-1}. This model generally underestimates the rate of collisions since it fails to account for electrostatic attractive forces between particles and thus should be regarded as a lower limit for k_{col}. More accurate descriptions of intermolecular interactions come from Lennard-Jones potentials for nonpolar molecules and from Sutherland potentials for polar molecules. For comparison purposes with published data, we have used a Lennard-Jones collision rate constant of k_{LJ} = 8.3 × 10^{-10} cm^3 molecule^{-1} s^{-1} for pyrazine and water at $T = 298$ K. Energy transfer probabilities have been calculated using both hard sphere and Lennard-Jones collision rates and these probabilities are tabulated alongside the rate constants in Table 2. The integrated hard sphere probability for excitation of H_2O-(010) is 0.015 and the integrated Lennard-Jones probability is 0.006. That is, about one in 67 hard sphere collisions, or about one in 168 Lennard-Jones collisions, result in energy transfer into $H_2O(010)$ rotational states with $E_{rot} \leq 811$ cm^{-1}.

5. Collisional excitation of the H_2O (100) and (001) States. In addition to investigating energy gain into the $H_2O(010)$ state, we attempted to observe transient absorption signals corresponding to appearance of other vibrationally excited states of water. We looked for energy gain in the (100) state, corresponding to one quantum of excitation in the symmetric stretch mode (ν_1 = 3652 cm^{-1}), and the (001) state, with one quantum in the asymmetric stretch mode (ν_3 = 3756 cm^{-1}). The probe transitions to investigate these states were the (100) → (101) and (001) → (002) transitions, respectively. Within our ability to detect transient states of water, there was no apparent signal for either the (100) or (001) state. If collisions with highly excited pyrazine (E_{vib} = 37900 cm^{-1}) do result in excitation of these states, our unsuccessful attempts at detection yield an upper limit to the rate constants for energy gain into individual rotational levels corresponding to k_2^J(100, 001) ≤ 8 × 10^{-15} cm^3 molecule^{-1} s^{-1}. This result is significant since the energies

TABLE 2: State-Specific Bimolecular Rate Constants for Energy Gain in Vibrationally Excited Water (010) Formed via the Process:

$$\mathrm{Pyr}(E_{vib} = 37900\ \mathrm{cm}^{-1}) + \mathrm{H_2O} \xrightarrow{k_2^J} \mathrm{Pyr}(E_{vib} - \Delta E) + \mathrm{H_2O}(010, J_{KaKc})$$

$H_2O(010)$ J_{KaKc}[a]	transition frequency[b]	E_{rot}[c]	k_2^J, $\times 10^{-13}$ [d]	P_{HS}, $\times 10^{-4}$ [e]	P_{LJ}, $\times 10^{-4}$ [f]	ΔE[g]	$\langle \Delta E \rangle_{HS}$[h]	$\langle \Delta E \rangle_{LJ}$[h]
1_{01}	3782.180	23.811	3.4 ± 0.8	10	4.0	1550 ± 390	1.55	0.62
1_{10}	3729.256	45.760	2.8 ± 0.7	8.4	3.3	1570 ± 390	1.32	0.52
3_{03}	3818.775	137.150	1.9 ± 0.5	5.6	2.2	1660 ± 420	0.93	0.37
3_{13}	3671.929	144.737	0.6 ± 02	1.8	0.72	1670 ± 420	0.30	0.12
2_{21}	3731.351	147.559	1.6 ± 0.4	4.9	2.0	1670 ± 420	0.82	0.33
2_{20}	3728.861	148.744	0.5 ± 0.1	1.5	0.60	1680 ± 420	0.25	0.10
3_{21}	3654.321	224.589	1.6 ± 0.4	4.9	2.0	1750 ± 440	0.86	0.35
4_{23}	3841.648	313.269	1.4 ± 0.3	4.2	1.7	1840 ± 460	0.77	0.31
5_{05}	3850.307	326.021	1.0 ± 0.3	3.2	1.2	1850 ± 460	0.59	0.22
5_{32}	3716.019	535.747	0.8 ± 0.2	2.4	0.97	2060 ± 520	0.49	0.20
7_{07}	3590.432	585.896	0.7 ± 0.2	2.2	0.86	2110 ± 530	0.46	0.18
5_{50}	3700.154	811.396	0.5 ± 0.1	1.5	0.58	2340 ± 580	0.35	0.14

[a] States for which the sum of $K_a + K_c$ is odd (ortho states) have a nuclear spin degeneracy of $g = 3$. States for which $K_a + K_c$ is even (para states) have a nuclear spin degeneracy of $g = 1$. [b] Transition frequency in cm^{-1} for the transient IR probe of $H_2O(010,J_{KaKc})$. [c] The energy in cm^{-1} of the $H_2O(010)$ rotational state J_{KaKc} from ref 23. [d] Bimolecular rate constants k_2^J for the appearance of $H_2O(010,J_{KaKc})$ resulting from collisions with highly vibrationally excited pyrazine, in units of cm^3 $molecule^{-1}$ s^{-1}. [e] The hard sphere probability $P_{HS} = k_2^J/k_{HS}$ of energy gain into the J_{KaKc} state of $H_2O(010)$ is defined as the ratio of the energy transfer rate constant to the hard sphere collision rate constant k_{HS}. At $T = 300$ K, $k_{HS} = 3.3 \times 10^{-10}$ cm^3 $molecule^{-1}s^{-1}$ for pyrazine and water. [f] The Lennard-Jones probability $P_{LJ} = k_2^J/k_{LJ}$ of energy gain into the J_{KaKc} state of $H_2O(010)$ is defined as the ratio of the energy transfer rate constant to the Lennard-Jones collision rate constant k_{LJ}. At $T = 300$ K, $k_{LJ} = 8.3 \times 10^{-10}$ cm^3 $molecule^{-1}$ s^{-1}. [g] Total energy change defined as $\Delta E = \Delta E_{vib}(\mathrm{bath}) + \langle \Delta E \rangle_{rot} + \langle \Delta E \rangle_{trans}$, where $\Delta E_{vib}(\mathrm{bath}) = 1594$ cm^{-1}, and initial rotational and translational distributions are assumed to have a temperature of 300 K. [h] The average amount of energy lost per collision from hot pyrazine corresponding to energy gain in $H_2O(010,J_{KaKc})$. This value is determined by the product of ΔE for each state and its probability $\langle \Delta E \rangle_{col} = \Delta E P_{col}$. Note that the probability and the average amount of energy depends on one's choice of collision model. Here we present results using hard sphere (HS) and Lennard-Jones (LJ) collision models.

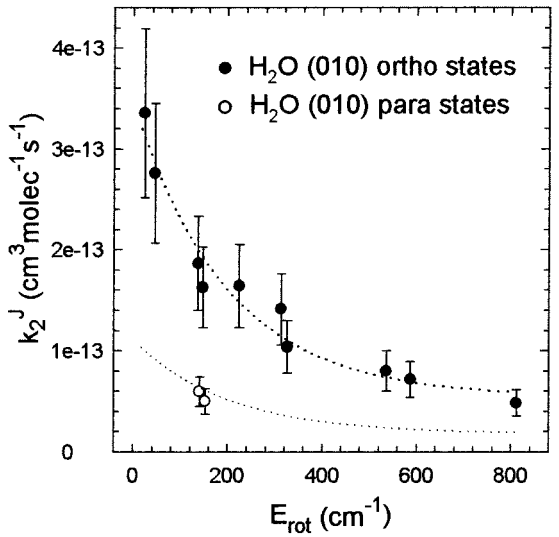

Figure 6. State-specific bimolecular rate constants for energy transfer from pyrazine with 37900 cm^{-1} vibrational energy to $H_2O(010,J_{KaKc})$ determined from population measurements made 1 μs after 266 nm uv excitation of pyrazine. Solid circles represent J_{KaKc} states with nuclear spin degeneracy of 3, open circles are states with nuclear spin degeneracy of 1. The dotted lines result from a Boltzmann fit of the experimental data. Error bars are 25%.

of the (100) and (001) states are larger than the energy of any single vibrational mode in pyrazine.

Discussion

From our state-resolved measurements, a clear picture of the vibrational energy gain in water emerges. Water molecules with one quantum of excitation in the ν_2 bending vibration, corresponding to an energy gain of 1594 cm^{-1}, result from collisions with highly excited pyrazine containing $E_{vib} = 37900$ cm^{-1}. These molecules are characterized by rotational excitation ($T_{rot} = 630$ K) and velocity distributions that are broadened ($T_{trans} \sim 500$ K) relative to the initial 298 K distribution. The energy transferred into the ν_2 bending mode is accompanied by rotational and translational excitation, but these energies are much smaller than the energy in the ν_2 mode. Thus, most of the energy acquired by water through this pathway is in the form of vibrational energy. From absolute rate measurements, we find that energy gain into the bending mode of water occurs once in 67 hard sphere collisions or once in 168 Lennard-Jones collisions. Within our experimental sensitivity, no evidence was found for collisional excitation of the higher frequency stretching modes in water at 3652 and 3756 cm^{-1}. We now discuss the implications of these results by first considering what is known about vibrational energy transfer from molecules with low initial amounts of energy.

It is well established for molecules with low levels of vibrational excitation that collisional energy loss can be mediated either through short-range repulsive intermolecular forces or through long-range attractive interactions.[2−4] In the Landau−Teller theory for molecular gases, loss of vibrational energy via collisions occurs through repulsive interactions and usually results in rotational and translational excitation of the recoiling molecules.[4] Vibrational energy exchange between collision partners can also result from impulsive collisions, with accompanying rotational and translational energy gain in the recoiling molecules but this process occurs with lower probabilities and is quite sensitive to the relative time scale of the various atomic and molecular motions. Mahan[25] predicted, and later Sharma and Brau[26,27] demonstrated theoretically, that pure vibrational energy transfer between two infrared active modes may occur through a different mechanism, namely that of long-range coupling between transition moments. In this case, the rotational energy gain is determined by selection rules identical to those for optical processes and there is minimal recoil velocity since repulsive interactions do not mediate the energy transfer. For pure dipole−dipole coupling, the allowed change in J, the total angular momentum, is $\Delta J = \pm 1$ and very little rotational excitation results from the vibrational energy transfer. The prob-

TABLE 3: Comparison of Rotational and Translational Energy Gain Magnitudes and Energy Transfer Rate Constants for Scattered H_2O and CO_2 Resulting from the Process: Pyrazine(E_{vib}) + B $\xrightarrow{k_2^J}$ Pyrazine(E_{vib}) + B*

B*	E_{vib}, cm^{-1}	T_{rot}, K	T_{trans}, K	ΔE_{total}[e]	$k_2$int, $\times 10^{-12}$ [f]	Z_{HS}(int)[g]	Z_{LJ}(int)[g]
$H_2O(000)$[a]	37900	920	550	~600	19	18	46
$H_2O(010)$[b]	37900	630	490	~1800	5.0	67	168
$CO_2(00^00)$[c]	37900	1190	2000−4000	2000−9000	14	25	44
$CO_2(00^01)$[d]	40700	330	370	2349	1.8	215	375
$CO_2(10^00_{R1})$[d]	40700	353	380	1388	2.0	194	337
$CO_2(10^00_{R2})$[d]	40700	394	410	1288	1.2	323	562
$CO_2(02^20)$[d]	40700	333	370	1337	6.6	59	102

[a] For $H_2O(000)$, data correspond to rotational states with 1000 $cm^{-1} < E_{rot} < 1800$ cm^{-1}. Taken from ref 5. [b] For $H_2O(010)$, data correspond to rotational states with $E_{rot} < 810$ cm^{-1}. The energy of the (010) is 1594 cm^{-1}. [d] For $CO_2(00^01)$, (10^00_{R1}), (10^00_{R2}), and (02^20) data correspond to rotational states with $J \leq 41$. Taken from refs 28 and 29. The energies of the (00^01), (10^00_{R1}), (10^00_{R2}), and (02^20) states are 2349, 1288, 1388, and 1337 cm^{-1}. [e] Energy transferred from hot pyrazine to the bath molecule, in cm^{-1}, estimated by $\Delta E_{total} = \Delta E_{vib}(bath) + (\langle E\rangle_{rot} + \langle E\rangle_{trans})^{final} - (\langle E\rangle_{rot} + \langle E\rangle_{trans})^{initial}$. [f] All integrated rate constants k_2^{int} (as defined in the text) have units of cm^3 $molecule^{-1}$ s^{-1}. [g] The collision number Z is defined $Z = k_{col}/k_2^{int}$ and corresponds to the number of collisions required for the specified energy transfer channel.

ability for long range energy transfer is enhanced when the energy gap between donor and acceptor vibrational modes is minimized and thus this type of energy transfer favors interaction of modes that are resonant or nearly so. As the energy gap increases, the probability for the near-resonant mechanism decreases and vibration to translation energy transfer becomes more important.

In the collisional relaxation of highly excited aromatic molecules in a CO_2 bath, the most extensive state-resolved studies to date have focused on the energy gain pathways in CO_2. Flynn and co-workers[16,17,28,29] have found two distinct mechanisms for the excitation of CO_2 resulting from collisions with highly excited pyrazine. Short-range encounters result primarily in rotationally and translationally excited CO_2 (00^00) which has no vibrational energy[16,17] and long-range near-resonant energy transfer populates CO_2 vibrational levels, (10^00, 02^20, and 00^01) with almost no rotational or translational excitation.[28,29] In collisions of highly excited pyrazine with water, however, we find substantial differences in the energy gain dynamics for both the vibrationally excited bend state, which is the focus of this study, and in the ground vibrationless state, which has already been reported.[5] The results for H_2O and CO_2 that scatter from hot pyrazine are summarized in Table 3. We have demonstrated that collisions that excite the bending vibration in water are accompanied by a considerable amount of rotational energy in the scattered water. There are several possible reasons for the observed dynamics, which we will now consider. It is possible that a purely long-range mechanism is not operative for quenching of pyrazine with water and that short-range repulsive forces are responsible for excitation of the bending mode in water. This would account for the enhanced rotational energy of the (010) state. The lack of translational energy in the scattered vibrationally hot water might be viewed as inconsistent with a short-range impulsive mechanism, but there is evidence from our earlier studies on the scattering of the $H_2O(000)$ state that impulsive collisions involving water do not involve high recoil velocities. We believe this is a result of rotational shielding, wherein the low moments of inertia in water cause rotation to be faster than relative translation between collision partners. In this situation, energy from the collision goes preferentially into rotation of the recoiling molecules, rather than into translation. Cottrell first suggested this idea in the form of a rotational adiabaticity parameter[30] and Moore presented convincing experimental evidence that molecules containing two or more hydrogen atoms and small amounts of vibrational energy exhibit relative quenching probabilities that are well described by vibration-to-rotation energy transfer.[31] Rapid rotation in water, relative to translation, would effectively reduce the probability for long-range energy transfer since the transition matrix element depends on the relative orientation of the collision partners. It is also possible that both long-range and short-range interactions are active in the vibrational excitation of water but that the short-range mechanism occurs with higher probability and overshadows the contribution of the long-range mechanism.

In Table 3, the energy gain probabilities for a number of energy flow pathways from hot pyrazine into CO_2 and H_2O are compared. We find that the collision number for vibrational excitation of the $H_2O(010)$ state is larger than that for the H_2O (000) and $CO_2(00^00)$ states but quite a bit smaller than for the $CO_2(00^01)$ and (10^00) states, where the energy transfer is dominated by long-range interactions. It is interesting to note from the data in Table 3 that energy gain in the $CO_2(02^20)$ state also occurs via a long-range mechanism, but with a probability that is large relative to that for the $H_2O(010)$ state and the other CO_2 vibrational states. This is accounted for in part by the fact that the (02^20) state has twice as many rotational states as do the $CO_2(10^00)$ r1 and r2 states, which only contain the even rotational levels. Flynn and co-workers[29] also point out that the square of the quadrupole transition matrix element for the CO_2-(02^20) state is larger than for the other states in CO_2. In addition, there is a near-resonant donor vibration in pyrazine at 1346 cm^{-1}, resulting in a favorably small energy gap of $\Delta E \sim 10$ cm^{-1} for the excitation of the $CO_2(02^20)$ state.

We have a number of experiments planned to help clarify the role of rotation and vibration in the quenching of highly excited molecules. Temperature-dependent studies should provide insight into the relative contribution of long and short range interactions in generating vibrationally hot water. Studies on deuterated water will permit us to lower the rotational time of the bath molecule without influencing the electrostatic interactions or the collision rates. Additionally, quenching studies with other hydrogen containing bath species will help elucidate the role of rotation in the relaxation of highly excited molecules.

Conclusions

We have used high resolution transient infrared probing to measure the complete energy profile for vibrationally excited water molecules that result from collisions with highly excited pyrazine ($E_{vib} = 37900$ cm^{-1}). Vibrational excitation is found in the ν_2 bending mode at 1594 cm^{-1}, but not in the ν_1 and ν_3 modes at 3652 and 3756 cm^{-1}, suggesting that the vibration−vibration energy transfer from hot pyrazine to water is dominated by one-quantum transitions in the hot donor. Both rotational and translational excitation is present in the vibrationally excited,

scattered water molecules, but the rotational component is more pronounced than the recoil between collision partners. We believe that the observed energy gain profiles result from short-range collisions with highly excited pyrazine and that energy gain in rotation is larger than in translation due to the relatively fast rotational times for water. These studies highlight the importance of the bending vibration of water in the collisional quenching of highly excited pyrazine and demonstrate how the identity of the bath molecule can significantly influence the relaxation dynamics.

Acknowledgment. We gratefully acknowledge research support from the National Science Foundation (CHE-9624533) and equipment support from the Office of Naval Research (N00014-96-1-0788). A.S.M. is a Camille Dreyfus Teacher Scholar and was supported by a Clare Boothe Luce Professorship from the Henry Luce Foundation (1994−1999). R.L.S. received research support from the Boston University Undergraduate Research Opportunities Program.

References and Notes

(1) Gilbert, R. G.; Smith, I. W. M. *Theory of Unimolecular and Recombination Reactions*; Blackwell Scientific Publications: Oxford, 1990.

(2) Cottrell, T. L.; McCoubrey, J. C. *Molecular Energy Transfer in Gases*; Butterworth Scientific: London, 1961.

(3) Keeton, R. G.; Bass, H. E. *J. Acoust. Soc. Am.* **1976**, *60*, 78.

(4) Yardley, J. T. *Introduction to Molecular Energy Transfer*; Academic: New York, 1980.

(5) Fraelich, M.; Elioff, M. S.; Mullin, A. S. *J. Phys. Chem. A* **1998**, *102*, 9761.

(6) Elioff, M. S.; Fraelich, M.; Sansom, R. L.; Mullin, A. S. *J. Chem. Phys.* **1999**, *111*, 3517.

(7) Barker, J. R.; Toselli, B. M. *Int. Rev. Phys. Chem.* **1993**, *12*, 305.

(8) Hippler, H.; Troe, J. Recent Direct Studies of Collisional Energy Transfer in Vibrationally Highly Excited Molecules in the Ground Electronic State. In *Bimolecular Collisions*; Ashfold, M. N. R., Baggott, J. E., Eds.; Royal Society of Chemistry: London, 1989.

(9) Heymann, M.; Hippler, H.; Plach, H. J.; Troe, J. *J. Chem. Phys.* **1987**, *87*, 3867.

(10) Hippler, H.; Otto, B.; Troe, J. *Ber. Bunsen-Ges. Phys. Chem.* **1989**, *93*, 428.

(11) Rossi, M. J.; Pladziewicz, J. R.; Barker, J. R. *J. Chem. Phys.* **1983**, *78*, 6695.

(12) Yerram, M. L.; Brenner, J. D.; King, K. D.; Barker, J. R. *J. Phys. Chem.* **1990**, *94*, 6341.

(13) Toselli, B. M.; Walunas, T. L.; Barker, J. R. *J. Chem. Phys.* **1990**, *92*, 4793.

(14) Elioff, M. S.; Wall, M. C.; Lemoff, A. S.; Mullin, A. S. *J. Chem. Phys.* **1999**, *110*, 5578.

(15) Wu, F.; Weisman, R. B. *J. Chem. Phys.* **1999**, *110*, 5047.

(16) Mullin, A. S.; Park, J.; Chou, J. Z.; Flynn, G. W.; Weston, R. E. *Chem. Phys.* **1993**, *175*, 53.

(17) Mullin, A. S.; Michaels, C. A.; Flynn, G. W. *J. Chem. Phys.* **1995**, *102*, 6032.

(18) Wall, M. C.; Mullin, A. S. *J. Chem. Phys.* **1998**, *108*, 9658.

(19) Knee, J.; Johnson, P. *J. Phys. Chem.* **1985**, *89*, 948.

(20) Dietz, T. G.; Duncan, M. A.; Puiu, A. C.; Smalley, R. E. *J. Phys. Chem.* **1982**, *86*, 4028.

(21) Yamazaki, I.; Sushida, K.; Baba, H. *J. Chem. Phys.* **1979**, *71*, 381.

(22) Nelson, D. D.; Schiffman, A.; Lykke, K. R.; Nesbitt, D. J. *Chem. Phys. Lett.* **1988**, *153*, 105.

(23) Air Force Research Labs, HITEMP Spectroscopic Database, 1998.

(24) Herzberg, G. *Molecular Spectra and Molecular Structure II: Infrared and Raman Spectra*; Van Nostrand Reinhold: New York, 1945.

(25) Mahan, B. H. *J. Chem. Phys.* **1967**, *46*, 98.

(26) Sharma, R. D. *Phys. Rev.* **1969**, *177*, 102.

(27) Sharma, R. D.; Brau, C. A. *J. Chem. Phys.* **1969**, *50*, 924.

(28) Michaels, C. A.; Mullin, A. S.; Flynn, G. W. *J. Chem. Phys.* **1995**, *102*, 6682.

(29) Michaels, C. A.; Mullin, A. S.; Park, J.; Chou, J.; Flynn, G. W. *J. Chem. Phys.* **1998**, *108*, 2744.

(30) Cottrell, T. L.; Robbie, R. C.; McLain, J.; Read, A. W. *Trans. Faraday Soc.* **1964**, *60*, 241.

(31) Moore, C. B. *J. Chem. Phys.* **1965**, *43*, 2979.